Composites Part C: Open Access 18 (2025) 100643

Contents lists available at ScienceDirect

Composites Part C: Open Access

journal homepage: www.sciencedirect.com/journal/composites-part-c-open-access

Thermoset (epoxy) - thermoplastic (polyetherimide) carbon fiber reinforced laminates featuring improved crack resistance in double cantilever beam tests due to hybridization

Kay A. Weidenmann [a,b,*], René Alderliesten [b], Julie J.E. Teuwen [b]

[a] University of Augsburg, Institute of Materials Resource Management (MRM), Germany
[b] Delft University of Technology, Aerospace Structures and Materials (ASM), Netherlands

ARTICLE INFO

Keywords:
DCB test
Carbon fiber reinforced polymers
Hybrid laminates
Crack propagation

ABSTRACT

Fiber-metal laminates are a well-known and established material concept featuring an enhanced crack propagation resistance when compared to their metal and fiber reinforced plastic (FRP) constituents. In this paper, this approach is transferred to purely carbon fiber reinforced plastic (CFRP) based laminates made from layers having polyetherimide (PEI) and epoxy matrices in an alternating laminate architecture. The laminates are manufactured via hot pressing. Double-cantilever beam (DCB) tests are performed on standard samples for both the hybrid laminates in different configurations as well for the both constituent materials, i.e. carbon fiber reinforced PEI (CFR-PEI) and carbon fiber reinforced epoxy. As the formation of an interphase is already reported in literature for this matrix combination, microstructural investigations have also been carried out in addition to fractography on crack surfaces. It is shown that the hybrid materials outperform both constituents regarding the crack resistance when crack initiation starts in the tougher CFR-PEI layer and the laminate layup is 0/90°. In the other configurations investigated, there is no significant effect. The energy dissipating mechanisms are crack jumping and the formation of several parallel cracks. Consequently, crack resistance in such hybrids might be controlled in future by adjusting the crack resistance of the constituents as well as the laminate architecture.

1. Introduction

Fiber-metal laminates based on aluminum and glass fiber reinforced plastics (GFRP) have been invented in the 1980s and reveal outstanding fatigue crack resistance and impact resistance [1], which is why this material class has been introduced in aircraft structures [2]. In the last decades, CFRP materials also made their way into aircraft structures as well as hybrid laminates based on aluminum (Al) and CFRP [3], named CARALL (carbon fiber reinforced aluminum laminates). One major shortcoming of CARALL laminates is the reduced corrosion resistance. Wu et al [4] report a reduction of the interlaminar shear strength in the range of 70 % for such a material system due to galvanic corrosion when immersed in electrolytic solution. Consequently, alternative hybrid laminates are sought for that combine the advantages proven for Al-GFRP laminates but overcoming the shortcomings that are evident when materials with a high difference in corrosion potential are used. One approach is the introduction of isolating interlayers [5] or a surface treatment of the aluminum reducing the difference in corrosion potential. Common approaches are chemical conversion or sol-gel processes leading to thin interlayers. An overview on these approaches is given by [6]. Furthermore, replacing aluminum by titanium (Ti) resulting in Ti-CFRP laminates also improves the corrosion behavior [7]. Nevertheless, titanium is a relatively expensive material with a lower lightweight potential than aluminum under bending load, which is a crucial load case for laminates.

Consequently, an alternative approach would be to replace the metal component in fiber-metal laminates (FML) by a different FRP material to enhance the crack propagation behavior. In this regard, Rzeczkowski et al. have shown that GFRP-CFRP laminates outperform their constituents regarding the G_{IC} values measured in double cantilever beam (DCB) test. The increase was explained by the synergy between GFRP and CFRP having different stiffness as well as mixed-modes and fiber bridging phenomena [8].

In the last years, several reports had a closer look at bringing thermosets and thermoplastics together. Bauer et al. used continuously fiber reinforced epoxy to locally reinforce short fiber reinforced

* Corresponding author.
E-mail address: kay.weidenmann@mrm.uni-augsburg.de (K.A. Weidenmann).

https://doi.org/10.1016/j.jcomc.2025.100643

Available online 19 August 2025

thermoplastics [9]. However, the constituents were not co-cured, but the epoxy-based components already had been cured prior to injection co-molding. The same is true for the investigations carried out by Yudhanto et al. [10] for adhesively bonded CFRP. Nevertheless, there are several reports on thermoplastic-epoxy interactions – recently reviewed by Deng et al. [11]. It is evident that the main motivation of co-curing of thermoplastics and thermosets has been the creation of a surface layer on the epoxy-based component that would allow for a subsequent welding process [12–14]. While most thermoplastics are not compatible to thermosets and do not interact, some promising candidates are polysulfone (PSU), polyethersulfone (PES), both used e.g. by [12], and polyetherimide (PEI). PEI forms an interphase with epoxy showing a particle-like microstructure gradually morphing from epoxy to PEI [15]. Beside the three mentioned, many others have been reported to be compatible with epoxy, but regarding the potential application in demanding structural applications, PSU, PES and PEI are the most promising candidates.

Consequently, there are some reports on PEI used for welding purposes to epoxy-based FRP [14,16,17]. All the reports describe the formation of the gradual interface, as mentioned above, between the constituents. Consequently, functionalizing epoxy-based composites with PEI has been used by Chen et al. [18] to optimize the fiber-matrix interaction. Regarding the resulting properties, PEI has proven to be a toughening agent for epoxy [19]. Building on this, various authors report on the use of carbon nanotube-modified PEI in particular as a thermoplastic interlayer to improve the mechanical properties of the primarily adhesive interlayer. These interlayers are used both in relatively brittle thermoplastics (e.g., PEEK) and in epoxy-based CFRP [20,21].

Interestingly, there are no reports to the knowledge of the authors, that tried to bring the concept of toughening CFRP with PEI interlayers to a both continuously fiber reinforced multilayer lay-up, i.e. to a material system that combines CFR-PEI with CFR-epoxy in a hybrid laminate to enhance fracture toughness. This would bring together the toughening effect of PEI for epoxy laminates and the toughening effect that has been reported for hybrid laminates in general with both constituents featuring a continuous fiber reinforcement offering load-carrying abilities.

This novel approach was chosen by the authors in the article at hand. Consequently, the aim of this contribution is to investigate the crack propagation in hybrid CFRP laminates with both continuously carbon fiber reinforced PEI- and epoxy-based layers in comparison to the behavior of the constituents. Alternating layers from CFR-PEI and CFR-epoxy allow for a formation of the interphases reported between each layer and establish the structural integrity of the overall laminate, although the consolidation is done following the consolidation cycle of the epoxy-based component without reaching the melting temperature of the CFR-PEI. In doing so, the material concept is quite similar to CARALL with the PEI replacing the aluminum layers and consequently overcome not only the corrosion issue but also providing a chemically bonded interface by forming an interphase.

2. Material and methods

2.1. Material

The materials used to manufacture the samples were unidirectional (UD) tape and prepreg materials, respectively. The tape used was a PEI-CF (V_f = 69 vol. %) tape provided by Cytec. The epoxy-based prepreg was HexPly 8552-IM7–33 %−134 (V_f = 67 vol. %). For the last-mentioned the miscibility with PEI has already been proven [22]. The nominal thickness after consolidation of the PEI-CF tape was approx. 200–250 μm, for the HexPly prepreg approx. 125 μm. Consequently, a pair of two HexPly layers should correspond to one layer of PEI-CF tape regarding the thickness, which is taken into account when defining the layup and is mirrored in the notation used in Table 1. This is why "double layers" occur in the notation for the thermoset (TS) layers which correspond to a single HexPly layer with a thickness of then approx. 200–250 μm. Furthermore, the notation should be read from the inlays to the outermost layers to get the symmetry of the laminate.

To investigate both the effects of fiber orientation and the matrix material, different layup configurations (cf. Table 1) have been manufactured by hot pressing. The laminates were laid up manually from manually cut sheets with the dimension of 300 × 300 mm². As the width of the tape and the prepreg were both 300 mm, each layer was formed by a complete tape or prepreg and contained no inner seams. For the layups solely manufactured from thermoplastics, consolidation took place at 17 bar and 320 °C for 30 mins. The heating/cooling ramp was 6 °C/min. During heating, the initial pressure was 2 bar. After 320 °C were reached, another dwell time of 10 mins was introduced before the consolidation process (17 bar, 320 °C for 30 mins) started.

The thermoset samples as well as the hybrid samples followed the consolidation cycle recommended by the manufacturer of the prepreg: after closing the mold, a pressure of 7 bar was continuously applied to the layup during the following steps. The layup was heated to 110 °C at a heating rate of 3 °C/min. After a dwell time of 60 mins, the layup was further heated to 180 °C at the same heating rate. At this consolidation temperature, the stack was kept for another 120 mins before cooling

Table 1
Tested laminate configurations. The lower case numbers indicate the number of repeating layers in the configuration given. "Inlay" names the position of the polyimide inlay in the layup, i.e. the symmetry layer of the whole stack. The notation should be read from the inlays to the outermost layers to get the symmetry of the laminate. The last line gives the approximate thickness of the consolidated plates. Color code in line 1: blue = thermoplastic laminates, green = thermoset laminates, orange = hybrid laminates.

TP 0/0°	TS 0/0°	TP 0/90°	TS 0/90°	H(TP) 0/0°	H(TP) 0/90°	H(TS) 0/90°
				$[0°0°]_1$ TS	$[90°90°]_1$ TS	$[90°]_1$ TP
				$[0°0°(TS)0°(TP)]_4$	$[90°90°(TS)0°(TP)]_4$	$[90°(TP)0°0°(TS)]_4$
$[0°]_{14}$ TP	$[0°]_{20}$ TS	$[90°0°]_7$ TP	$[90°90°0°0°]_5$ TS	$[0°]_1$ TP	$[0°]_1$ TP	$[0°0°]_1$ TS
Inlay	Inlay	Inlay	Inlay	Inlay	Inlay	Inlay
$[0°]_{14}$ TP	$[0°]_{20}$ TS	$0°90°]_7$ TP	$[0°0°90°90°]_5$ TS	$[0°]_1$ TP	$[0°]_1$ TP	$[0°0°]_1$ TS
				$[0°0°(TS)0°(TP)]_4$	$[90°90°(TS)0°(TP)]_4$	$[90°(TP)0°0°(TS)]_4$
				$[0°0°]_1$ TS	$[90°90°]_1$ TS	$[90°]_1$ TP
3.5 mm	**4.6 mm**	**3.9 mm**	**4.9 mm**	**4.1 mm**	**4.3 mm**	**4.3 mm**

down (still under constant pressure of 7 bar) to 40 °C at a cooling rate of 5 °C/min.

As the layups were designed for DCB tests, they all contained a local inlay made from polyimide foil in the plane of symmetry of the layup. The foil was pretreated with release agent (Marbocote 227) on both sides prior to the consolidation of the layup. The designation of the samples (see Table 1) is as follows: H (= hybrid) lay-up, TP (= thermoplastic) or TS (=thermoset) shows which material is at the interface of the crack initiation plane, 0/0 or 0/90 refers to the different fiber orientations: fully UD for 0/0, 0/90 with the UD layer at the interface and 90° layers following the stacking sequence shown in the table.

As layup configuration H(TP) 0/90° and H(TP) 0/0° contained two PEI-CF layers in direct contact at the center of the layup, a consolidation following the thermoset route would not lead to a consolidation at the center layer. Therefore, the two neighboring layers at the center including the inlay were pre-consolidated at 15 bars and 350 °C at 30 mins. The higher temperature accounted for the lower pressure which was used to prevent squeezing the layers what would have increased the width and fiber ondulations. Afterwards, the layup was completed and consolidated following the consolidation process described for the hybrids above.

The consolidation via hot pressing was performed on a 1000 kN hydraulic press (Joos LAP 100) under load control. As the consolidation had an influence on the final thickness of the consolidated plates, the number of layers was partially adopted. In doing so, all plates had a thickness in the range of 3.5 to 4.9 mm which is within the range of the standard used for testing (ISO 15024).

3. Methods

3.1. Sample preparation

After consolidation, the plates were cut using a semi-automated diamond blade cutter (CompoCut ACS300) using preset cutting parameters for CFRP at a laminate thickness of max. 5 mm. The specimen geometry followed the standard ISO 15024 for DCB tests. The overall length of the specimens was 200 mm, with the inlay occupying 60 mm. The width of the samples was 25 mm. The approximate thicknesses of the consolidated plates are given in Table 1. The exact values for each sample have been measured prior to the DCB test using a calliper.

For the DCB tests, loading blocks made from aluminium were glued on the samples with epoxy glue (Loctite 3425), which hardened at least 12 h at ambient temperature using a purpose-designed mold that was clamped mechanically. In doing so, a_0 was in the range of 44–46 mm and determined for each sample set.

3.1.1. DCB tests

DCB tests according to ISO 15024 were performed on a Zwick 1455 universal testing machine with a maximum load capacity of 20 kN and the corresponding load cell. The tests were monitored using a standard video camera automatically capturing an image every 2 s. The images were saved with a time stamp and correlated to the measured values. The crosshead velocity for the TP-samples was set to 5mm/min, for the TS- and the H-samples, the velocity was reduced to 2 mm/min. To follow the crack propagation, the samples were additionally continuously monitored using a magnifying glass. 23 markers at distances of 1, 2, 3, 4, 5, 6, 7, 8, 9, 10, 15, 20, 25, 30, 35, 40, 45, 50, 51, 52, 53, 54, 55 mm were put on the samples setting the trigger points for the crack propagation to be monitored. The test included an unloading-reloading cycle according to the standard to pre-crack the sample and define a proper initial state. If cracks were propagating too fast skipping markers, which rarely happened, the corresponding value was just left out. The tests ended after the crack reached the 55 mm mark. For every material configuration at least three valid tests were considered in the evaluation.

The tests were evaluated following the standard using an Excel sheet. Both CBT and MCC correction terms were applied for all the samples. As they did not show a significant difference, the MCC correction was chosen to be the basis for the results on display in this paper.

3.2. Microstructure analysis and fractography

To have a closer look at the microstructure as well as to investigate the damage evolution after the test, microscopy on both cross-sections as well as on the fractured surfaces have been performed. For the cross-sections, samples have been embedded in epoxy resins and grinded/polished.

To prevent an interaction between the sample and the embedding resin, a fast and cold curing resin (Kulzer Technovit 4071) has been used. Samples were prepared the following route: Grinding with SiC paper 320 for 1 min, grinding with SiC paper 1000 for 1 min, grinding with SiC paper 2000 for 1 min, polishing with diamond suspension (3 μm) for 4 min, polishing with diamond suspension (1 μm) for 2 min. For investigating the cross-sections of the hybrid laminates, these were etched by immersing the sample in pure N,N-DMF which serves as a solvent for the PEI matrix.

For samples that had been chosen to investigate the fractured surfaces, the loading blocks were removed by cutting the samples again with a diamond saw approx. at the position −10 mm and 60 mm relative to the initial position of the inlay. In doing so, the samples could be recovered as one piece. Afterwards, the crack was opened manually until the samples were separated. Both the lower and the upper cracked surface of a representative sample of each configuration was investigated using a scanning laser microscope (Keyence VK-X1000) as well as a light microscope (Keyence VR-5000) to investigate the cracked surface. The laser scanning microscope also allowed to register the roughness in a semi-quantitative manner. The cross-sections mentioned above were also investigated using the laser microscope.

4. Results and discussion

4.1. DCB tests

Fig. 1 shows the results of the DCB test for the different material configurations investigated. The G_{Ic} values calculated for every crack propagation position based on the MCC correction are plotted vs. a. The results were clustered in different classes and are represented by representative curves. From the diagrams, it is evident that the pure thermoset materials feature the lowest G_{Ic} values in the range of 200 to 300 J/m² remaining more or less constant along the travel of the crack. Furthermore, there is not a significant influence of the layup configuration, but it has to be mentioned, that the UD oriented layup (TS 0/0°) shows slightly higher values than the biaxial layup (TS 0/90°).

This effect is much more pronounced for the thermoplastic materials shown in the center of Fig. 1. Here we see a clear difference with the 0/90° layup featuring the lower crack resistance in comparison to the UD samples. The influence of the fiber architecture in epoxy-based CFRP has already been assessed by Rehan et al. [23]. In their study, the UD material outperformed the 0/90° configuration by an increase of 33 %. The average values here are 20 % higher for the UD configuration, which is in the same range. Additionally, the overall crack resistance for CF-PEI is at a much higher level with G_{Ic} values between 1000 and 1500 J/m².

From literature, it is well known that PEI is tougher than epoxy, that is the main motivation of this work, too. Frassine and Pavan [24] investigated a carbon fiber reinforced PEI composite with a fiber content of 58 ma %. They found G_{Ic} values in the range of 2100 J/m². This is significantly higher than the values derived in this study, but the fiber content of 58 ma. % reported by [24] corresponds to a fiber volume content of approx. 46 vol. % (calculated with a density of 2 g/cm³ for the carbon fiber and 1,27 g/cm³ for the PEI), while the material investigated in the study at hand has a fiber volume content of 69 vol. %. As the pure PEI has a much higher crack resistance (cf. also [24]), this difference might be due to the different fiber content. Akkerman et al. [25] also

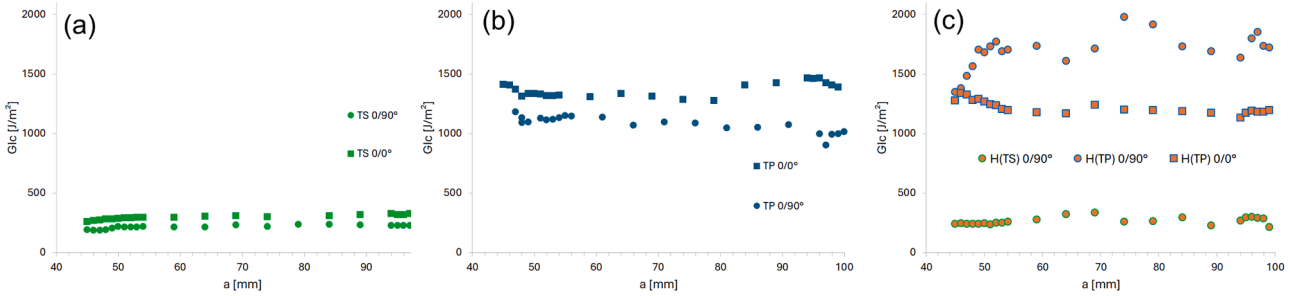

Fig. 1. Results of the DCB tests for representative specimens for the different composite configurations: pure thermoset samples (a), pure thermoplastic samples (b) and hybrid configurations (c).

investigated a CF-PEI laminate with a fiber content of 60 % and found values of G_{Ic} in the range of 1000 to 1200 J/m^2, which is in very good accordance to this study for both the fiber content and the values obtained. Indeed, they also discussed the difference to [24], but could not find an explanation themselves. Unfortunately, there is no reference published in open literature that assesses the influence of the fiber architecture on the crack resistance in CF-PEI laminates. When taking the findings of [23] into account, it is reasonable, that this effect is not depending on the matrix and should be found in CF-PEI, too – which is the case in the study at hand.

To sum up, it can be stated, that the results for both the pure materials, the TS and the TP laminates, are in very good agreement with literature.

For the hybrid laminates (H), there is a strong influence of the hybrid configuration on G_{Ic}. For H(TS) 0/90° having the starting crack between thermoset layers, the authors find no significant difference in the level of the G_{Ic} values. Fig. 2 shows indeed no obvious difference in the crack propagation behavior between TS 0/90° and the corresponding hybrid.

On the contrary, for hybrids with 0/90° architecture and starting cracks between thermoplastic layers (H(TP) 0/90°), there is a pronounced hybridization effect evident: The level of the G_{Ic} values are in average even higher than those of each constituent, outperforming the CF-PEI layups, especially when taking the fiber architecture into account.

This behaviour can be explained with the crack propagation that can be observed during the mechanical test. For both TS 0/0° and TS 0/90° the crack follows the interface where it had been initiated by the inserted inlay. This is also true for H(TS) 0/90° having the crack also initiated between two thermoset layers. For both TP 0/0° and TP 0/90° the crack also follows the interface where it had been initiated by the inserted inlay with only minor effects on the crack travel such as crack bridging. In contrast, H(TP) 0/90° shows various effects such like crack jumping between the interface where it was initiated and adjacent ones as well as the initiation of cracks on parallel interfaces – regularly starting at an early stage of the crack propagation. This difference is already evident when following the crack propagation during the DCB tests and are presented in Fig. 3.

Obviously, the conditions at the crack initiation interface play a decisive role: if the crack is initiated at an interface with a relative high propagation resistance, it is likely to swap to parallel interfaces featuring lower crack resistance which seems to be the case for interfaces partnered with thermoset layers. If the crack starts between two thermoset layers, it is already initiated at the weakest link in the composite hence remaining in this weak interface. Consequently, no mechanisms are initiated that would increase energy dissipation and consequently increasing the crack resistance represented by the G_{Ic} values. Indeed, Voleppe et al. [26] determined G_{Ic} values for the interface forming between unreinforced PEI foil and epoxy resin. Depending on the curing cycle, values were between approx. 420 and 880 J/m^2 for the epoxy-PEI interface in comparison to ca. 170 J/m^2 for the neat epoxy resin with the PEI/PEI interface being at 4000 J/m^2. From that it can be concluded that the CF-epoxy/CF-epoxy interface is the weakest also for the hybrid laminates at hand – as well as the CF-PEI/CF-PEI being the strongest – and the CF-PEI/CF-epoxy featuring intermediate values. Consequently, the crack prefers to switch to potentially weaker interfaces when initiated in the strongest one. Indeed, this effect is disappearing, when the fiber architecture in the hybrid is UD only: For H(TP) 0/0° the hybridization effect visible for H(TP) 0/90° cannot be detected anymore.

This is supported by the observations made during the test: the crack follows again the interface where it had been initiated without crack jumping and/or crack initiation on parallel interfaces as well as the G_{Ic} values remain more or less constant along the travel of the crack. This shows that the interface properties are not the only decisive factor but also the fiber orientation in neighboring layers. In H(TP) 0/90° the

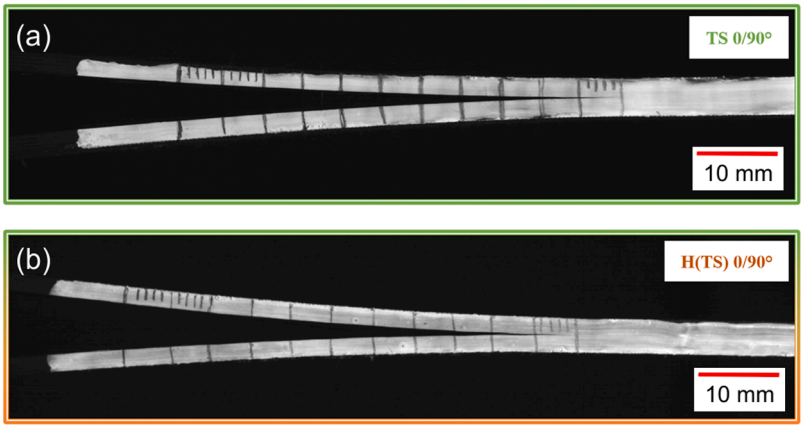

Fig. 2. Exemplary images of crack propagation during DCB tests for H(TS) 0/90° hybrid laminates (a) in comparison to TS 0/90° (b). There is no evidence for a change in crack propagation mechanism confirming the G_{Ic} values on a comparable level.

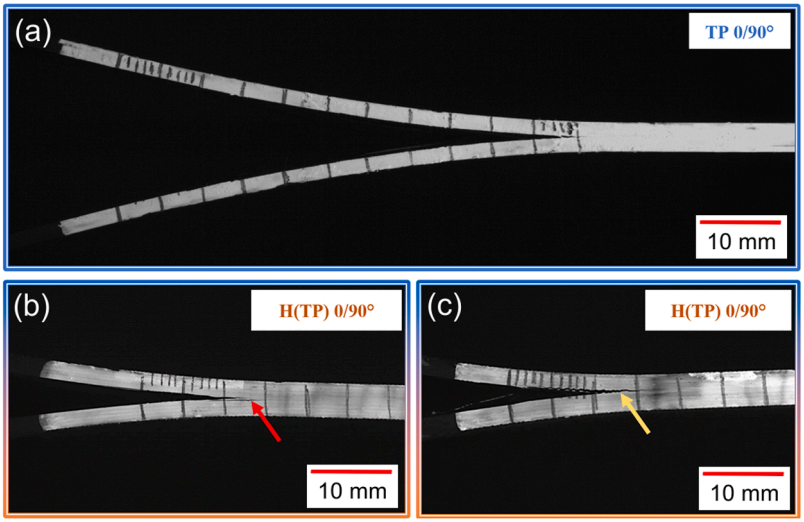

Fig. 3. Exemplary images of crack propagation during DCB tests for H(TP) 0°/90° hybrid laminates (b and c) in comparison to the corresponding sample TP 0°/90° (a). Forming of parallel cracks (b, red arrow) and crack jumping (c, yellow arrow) indicate a pronounced change in crack propagation mechanism at an early state of crack growth in comparison to the pure TP sample.

thermoset-based layers are mechanically matrix-dominated, which is not true for H(TP) 0/0°

Following the results observed for the non-hybrid composites, i.e. TP and TS laminates, the expectation would be that the 0/0° architecture outperforms the 0/90° configuration. This is definitely not the case with the average G_{Ic} level of H(TP) 0/0° being 20 % lower in comparison to H (TP) 0/90° It is also interesting to see that H(TS) 0/90° behaves like TS 0/90° and has the same characteristics as well as H(TP) 0/0° behaving like TP 0/0° with the G_{Ic} values still lower but on a comparable level. In contrast, H(TP) 0/90° has a pronounced hybridization effect.

Table 2 lists the average values of at least three valid samples for each configuration pointing out the differences discussed.

Indeed, from Table 2 another aspect that underlines the existence for a hybridization effect for H(TP) 0/90° only, showing an increase of 42 % for G_{Ic} in comparison to the initiation value while the other hybrid configurations have no significant change. Consequently, no significant increase in crack energy dissipation is taking place during the crack travel. Furthermore, it is obvious that all the configurations featuring neighboring TP layers at the level of crack initiation have the same level of $G_{Ic,0}$. The same is true for the crack being introduced between two thermoset layers. This means that for the crack initiation, the hybridization of the laminate plays no role.

The hybridization effect only occurs during the crack travel which is again in line with the observations made as it is necessary to initiate a crack before crack jumping, parallel cracks or fibre bridging may occur. Indeed, fiber bridging is partially also present in CF-PEI. This explains the relatively high increase for TP 0/0° and the slight increase in H(TP) 0/0° both showing this effect. Nevertheless, this effect pairs with crack jumping and the formation of parallel cracks in H(TP) 0/90° only.

4.2. Microstructure analysis and fractography

The investigation on the pristine cross-sections focussed on the hybrid samples to answer the question whether the interface reported in literature also forms in hybrid laminates. Indeed, this is the case for all the hybrids investigated. Furthermore, fiber orientation plays no role. Representative examples are shown in Fig. 4.

The thickness of the interface is in the range of 5 μm for all configurations which is less than the 9–10 μm reported by [27] using a comparable curing cycle but not the same epoxy system. Furthermore, [27] used a pure PEI film and not a CF-PEI tape. The same is true for Bruckbauer et al., who subdivide the interphase into three layers (an epoxy-dominated, a PEI-dominated and a bi-continuous phase) with the bi-continuous phase being in the range of 5 μm [28]. In preliminary work of one of the authors, a thickness of 70–80 μm at 180 °C processing temperature is reported [29], but these experiments were based on the corresponding resins in the A-stage, not in the B-stage like in the study at hand and in line with [27] and [28]. Indeed, for a B-stage, diffusion activity during curing might be less due to higher molecular weights of the ingredients. Nevertheless, the formation of the interface is clearly taking place as in diffusion inside the TP layer what is again confirming the state of the art [27–29].

For the investigation on the fracture behaviour, cross-sections of H (TP) 0/90° and H(TP) 0/0° samples at the crack tip region of DCB tested samples were chosen and presented in Fig. 5. It is clearly visible, that the crack in H(TP) 0/90° has left the interface where it was initiated, which is a further indicator for the crack jumping observed during the test. Furthermore, secondary cracks are visible. For H(TP) 0/0° the main crack was constantly travelling along the interface where it started.

The fractured surfaces clearly indicate a difference in crack

Table 2
Average G_{Ic} values for the different configurations evaluated in comparison to $G_{Ic,0}$. The G_{Ic} values themselves are calculated as the average along the crack travel, while G_{Ic},0 is the initial value when crack initiation has been detected (NL point).

	TP 0/0°	TS 0/0°	TP 0/90°	TS 0/90°	H(TP) 0/0°	H(TP) 0/90°	H(TS) 0/90°
G_{Ic} [J/m²]	1488±107	288±12	957±25	235±15	1226±38	1537±156	286±17
$G_{Ic,0}$ [J/m²]	1214±129	293±10	1148±59	225±18	1118±50	1081±182	262±18
$G_{Ic}/G_{Ic,0}$	1,23	0,98	0,83	1,04	1,10	1,42	1,09

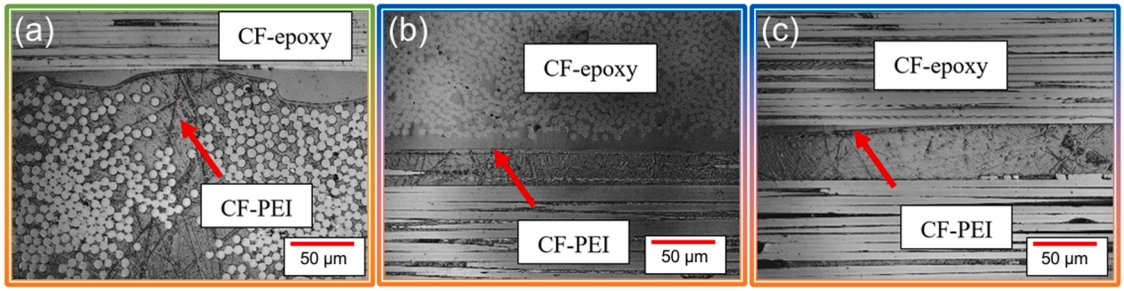

Fig. 4. Cross-sections of H(TS) 0/90° (a), H(TP) 0/90° (b) and H(TP) 0/0° (c). Red arrows mark the interphase formed between the PEI and the epoxy matrix.

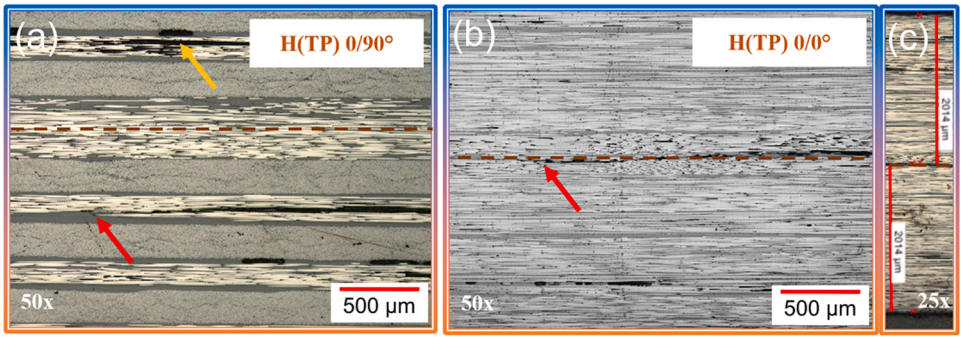

Fig. 5. Cross-sectional view at the end of the tip (red arrows) of the main crack in a H(TP) 0/90° sample (a) in comparison to a H(TP) 0/0° sample (b). An exemplary secondary crack is marked by a yellow arrow. The interface of crack initiation is marked by a dashed line. The annex (c) to image (b) shows the position of the main crack in H(TP) 0/0° in relation to the edges of the sample.

propagation behaviour (cf. Fig. 6). Only for the HS (TP) 0/90° configuration the crack propagates in a way that the neighboring 90° layer becomes visible on the cracked surface. The other samples reveal a relatively smooth surface when compared to H(TP) 0/90°. TS 0/90° and TP 0/90° seem to be smoother when compared to TS 0/0° and TP 0/0°, respectively.

As the laser scanning microscope used allowed for a semi-quantitative measurement of the surface roughness of the samples, this was done to confirm the impression from visual inspection. For each spot marked in Fig. 6, measurements along 29 lines were assessed and averaged. As the R_z is more sensitive to single grooves (compared to R_a), which are resulting on the cracked surface from crack jumping and the formation of parallel cracks, this value is taken for comparison. The values are given in Table 3.

Again, these values can be clearly correlated to the fractured surfaces displayed in Fig. 6 and the G_{Ic} values derived from the DCB experiments: High values for the roughness – especially when combined with high fluctuations – correlate to high G_{Ic} values as for TP0/0° and H(TP) 0/90°

All other samples show a relatively smooth cracked surface with R_z values being on a more or less constant level of 180 to 280 µm. Indeed, the difference between the 0/90° and 0/0° configuration for both TP and TS can also clearly be seen for the roughness values. This again confirms the fact that for composite laminates crack propagation behavior may differ depending on the laminate architecture as stated by [24].

When looking at the cracked surface of H(TS) 0/90° in comparison to H(TP) 0/90° both shown in Fig. 7, it is evident, that the formation of grooves on the fractured surfaces is also present in some small areas of H (TS) 0/90° Nevertheless, the crack here does not reach the adjacent thermoplastic layer or the interface inbetween, which is clearly indicated by the fiber orientation visible in the grooves. This in contrast to H (TP) 0/90°, where groove formation is much more pronounced (cf. Fig. 6) and the crack does reach the adjacent thermoset layer featuring a 90° fiber orientation. The pronounced crack formation is mirrored in the high values of R_z even increasing along the crack travel corresponding to the high G_{Ic} values and underlining the hybridization effect.

Indeed, this effect may also come from the fact, that the epoxy-based

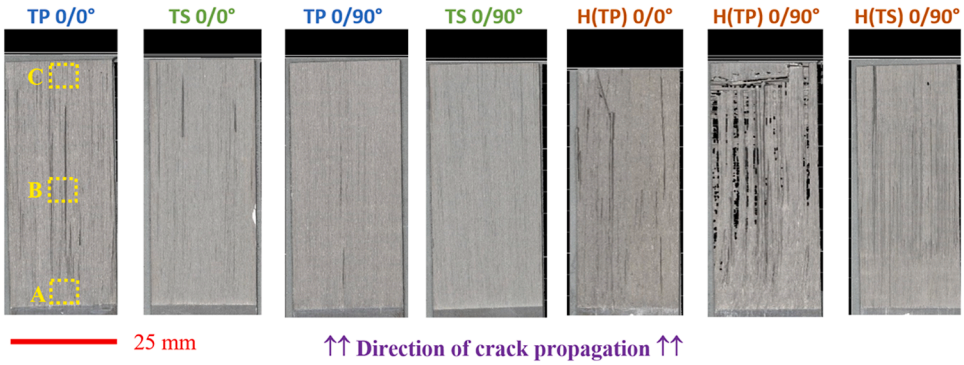

Fig. 6. Fractography of tested laminate configurations: view on the upper half of the cracked sample. Width of every sample displayed is 25 mm. Black spots in H(TP) 0/90° indicate the visibility of the 90° TS layer. The yellow squares mark the positions of the roughness measurements (see below).

Table 3
Roughness (R_z) values measured at three different positions (marked in Fig. 6) along the crack travel for all sample configurations investigated.

	TP 0/0°	TS 0/0°	TP 0/90°	TS 0/90°	H(TP) 0/0°	H(TP) 0/90°	H(TS) 0/90°
R_z (Pos.A) [µm]	229.5±71	191.8±26	207.7±16	185.7±25	256.7±25	294.0±52	168.7±40
R_z (Pos.B) [µm]	647.6±47	276.4±16	235.7±26	185.1±24	239.5±36	705.5±33	195.3±26
R_z (Pos.C) [µm]	392.1±172	196.1±25	246.2±17	179.4±15	207.8±29	929.8±63	233.4±14

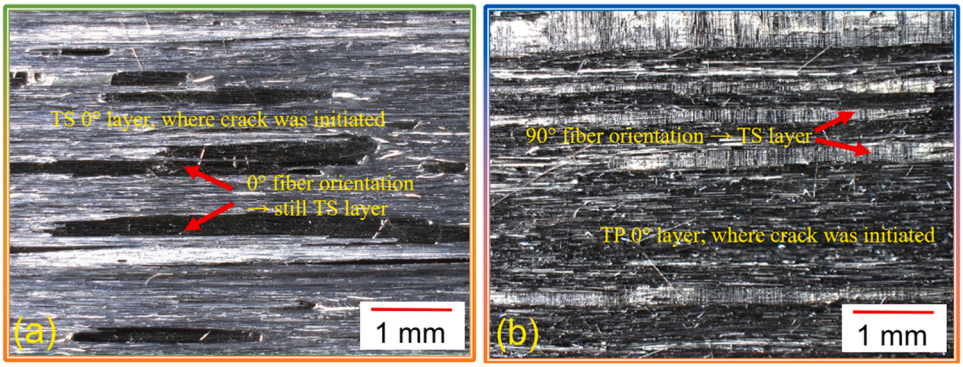

Fig. 7. Fractography of tested laminate configurations: view on the upper half of the cracked sample. In H(TS) 0/90° the crack does not reach the adjacent TP layer (a), which is clearly the case for H(TP) 0/90° (b).

prepregs had to be doubled to get the same thickness as for the CF-PEI layers. Consequently, there is an "inner" interface existent for the TS layers only. Still, the grooves indicating the travel of the crack to adjacent layers is very rare for H(TS) 0/90° which coincides with the low roughness and G_{Ic} values.

To sum up, it can be stated that the results from the fractographic investigations are well in line with the results from the DCB tests and confirm the findings discussed regarding the hybridization effect.

5. Summary and conclusions

The aim of this contribution was to investigate the crack propagation in hybrid CFRP laminates with PEI- and epoxy-based continuous fiber-reinforced layers in comparison to the behavior of both CFRP constituents. It can be stated, that a hybridization effect, i.e. the hybrid surpassing the properties of both the constituents, can clearly be seen for distinct laminate configurations when the starting crack is initiated between two CF-PEI layers and the stacking sequence is 0/90°. For this case, the G_{Ic} values even exceed the level of the single constituents by approx. 60 % (when compared to the TP 0/90° configuration) and even by approx. 550 % (when compared to the TS 0/90° configuration). The effects are based on a change in crack propagation mechanisms, based on crack jumping between different interfaces as well as the initiation of parallel cracks, which could be proven by means of fractography as well as observing the crack travel during the DCB experiments. The following conclusions can be drawn:

- Based on thermoplastics compatible to epoxy systems, hybrid laminates can be consolidated following the epoxy consolidation route as long as alternating layer architecture is chosen. Otherwise, a pre-consolidation of neighboring thermoplastic layers is necessary.
- The hybridization effect is depending on an alternating layup of the thermoset-/thermoplast-based laminates.
- The hybridization effect is based on a change in crack propagation, in detail by triggering crack jumping and crack initiation in parallel interfaces.
- The hybridization effect is not occurring, when the crack is initiated in the weakest interface present, but pronounced, when the crack is initiated in the strongest interface.
- The fiber orientation in the hybrids plays a role for the existence of a hybridization effect, too, as can be seen from the characteristics given in Table 2. Consequently, the hybridization effect in such hybrid laminates might be controlled by interface design and laminate architecture.

The investigations at hand show, that fiber reinforced hybrid laminates based on continuously fiber-reinforced thermoset and thermoplastic matrices represent a promising material concept, that offer high lightweight potential and overcome disadvantages that are observed in fiber-metal laminates. Manufacturing follows a well-established route and might even be automated in fiber placement processes as the laminates are based on well-established prepregs or tapes. In doing so, the material has the perspective to become a purely CFRP-based successor of CARALL or other fiber-metal laminates.

Nevertheless, it has to be pointed out that not every hybrid laminate investigated in this study showed improved crack resistance. The effect is strongly based on the location of crack initiation, which is done in a controlled manner here. Consequently, to transfer this knowledge to laminates under near-service loads, other crack-initiating mechanisms such like fatigue and impact behavior are still to be investigated.

CRediT authorship contribution statement

Kay A. Weidenmann: Writing – original draft, Investigation, Formal analysis, Data curation, Conceptualization. **René Alderliesten:** Writing – review & editing, Resources, Methodology, Conceptualization. **Julie J. E. Teuwen:** Writing – review & editing, Resources, Methodology, Conceptualization.

Declaration of competing interest

The authors declare the following financial interests/personal relationships which may be considered as potential competing interests:

Kay A. Weidenmann reports equipment, drugs, or supplies was provided by Delft University of Technology. If there are other authors, they declare that they have no known competing financial interests or personal relationships that could have appeared to influence the work reported in this paper.

Acknowledgement

The research work presented has been carried out at TU Delft during a research stay of the corresponding author, who wants to thank for the hosting. The authors also kindly acknowledge Paul Poupot, SeaTech Ecole d'Ingénieurs, Toulon (France) for assisting in the mechanical experiments during his internship at TU Delft. This research did not receive any specific grant from funding agencies in the public, commercial, or not-for-profit sectors.

Data availability

Data will be made available on request.

References

[1] M. Sadighi, R.C. Alderliesten, R. Benedictus, Impact resistance of fiber-metal laminates: a review, Int. J. Impact. Eng. 49 (2012) 77–90.
[2] A. Vlot, L.B. Vogelesang, T.J. De Vries, Towards application of fibre metal laminates in large aircraft, Aircr. Eng. Aerosp. Technol. 71 (6) (1999) 558–570.
[3] E.C. Botelho, R.A. Silva, L.C. Pardini, M.C. Rezende, A review on the development and properties of continuous fiber/epoxy/aluminum hybrid composites for aircraft structures, Mater. Res. 9 (2006) 247–256.
[4] X.T. Wu, L.H. Zhan, M.H. Huang, X. Zhao, X. Wang, G.Q. Zhao, Corrosion damage evolution and mechanical properties of carbon fiber reinforced aluminum laminate, J. Cent. South. Univ. 28 (3) (2021) 657–668, 2021.
[5] M. Stoll, F. Stemmer, S. Ilinzeer, K.A. Weidenmann, Optimization of corrosive properties of carbon fiber reinforced aluminum laminates due to integration of an elastomer interlayer, Key. Eng. Mater. 742 (2017) 287–293.
[6] G.W. Critchlow, D.M. Brewis, Review of surface pretreatments for aluminium alloys, Int. J. Adhes. Adhes. 16 (4) (1996) 255–275.
[7] M. Ostapiuk, J. Bieniaś, Corrosion resistance in NaCl environment of fiber metal laminates based on aluminum and titanium alloys with carbon and glass fibers, Adv. Eng. Mater. 23 (3) (2021) 2001030.
[8] J. Rzeczkowski, S. Samborski, K. Prokopek, Experimental determination of the mode I fracture toughness in FRP laminates with hybrid delamination interfaces, Adv. Sci. Technol. Res. J. 16 (5) (2022) 129–135.
[9] P. Bauer, Y.N. Becker, N. Motsch-Eichmann, K. Mehl, I. Müller, J. Hausmann, Hybrid thermoset-thermoplastic structures: an experimental investigation on the interface strength of continuous fiber-reinforced epoxy and short-fiber reinforced polyamide 6, Open Access 3 (2020) 100060.
[10] A. Yudhanto, M. Almulhim, F. Kamal, R. Tao, L. Fatta, M. Alfano, G. Lubineau, Enhancement of fracture toughness in secondary bonded CFRP using hybrid thermoplastic/thermoset bondline architecture, Compos. Sci. Technol. 199 (2020) 108346.
[11] S. Deng, L. Djukic, R. Paton, L. Ye, Thermoplastic–epoxy interactions and their potential applications in joining composite structures–a review, Appl. Sci. Manuf. 68 (2015) 121–132.
[12] A.R. Wedgewood, P.E. Hardy, Induction welding of thermoset composite adherends using thermoplastic interlayers and susceptors, Technol. Transf. Glob. Comm. (1996) 850–861.
[13] A. Beehag, P. Falzon, R. Paton, A Mouldable Thermoplastic Interface For Advanced Composite Components to Reduce Costs in Aircraft Assembly, SAE Technical Paper, 2005, 2005-01-3310.
[14] E. Tsiangou, S.T. de Freitas, I.F. Villegas, R. Benedictus, Investigation on energy director-less ultrasonic welding of polyetherimide (PEI)-to epoxy-based composites, Compos. B 173 (2019) 107014.
[15] B. Lestriez, J.P. Chapel, J.F. Gérard, Gradient interphase between reactive epoxy and glassy thermoplastic from dissolution process, reaction kinetics, and phase separation thermodynamics, Macromolecules 34 (5) (2001) 1204–1213.
[16] C. Ageorges, L. Ye, Resistance welding of thermosetting composite/thermoplastic composite joints, Appl. Sci. Manuf. 32 (11) (2001) 1603–1612.
[17] C. Brauner, S. Nakouzi, L. Zweifel, J. Tresch, Co-curing behaviour of thermoset composites with a thermoplastic boundary layer for welding purposes, Adv. Compos. Lett. 29 (2020) 2633366X20902777.
[18] S. Chen, J. Feng, Epoxy laminated composites reinforced with polyethyleneimine functionalized carbon fiber fabric: mechanical and thermal properties, Compos. Sci. Technol. 101 (2014) 145–151.
[19] A. Murakami, D. Saunders, K. Ooishi, T. Yoshiki, M. Saitoo, O. Watanabe, M. Takezawa, Fracture behaviour of thermoplastic modified epoxy resins, J. Adhes. 39 (4) (1992) 227–242.
[20] Y.H. Kim, S. Kumar, X. Li, S.Y. Kim, D.H. Shin, Temperature-dependent mechanical properties and material modifications of carbon fiber composites for optimized structures in high-end industrial applications, Compos. B 303 (2025) 112602.
[21] L.L. Zhang, X.L. Li, P. Wang, X.H. Wei, D.Q. Jing, X.H. Zhang, S.C. Zhang, Increasing the interlaminar fracture toughness and thermal conductivity of carbon fiber/epoxy composites interleaved with carbon nanotube/polyimide composite films, New Carbon Mater. 38 (2023) 566–573 [3].
[22] D. Quan, D. Yue, Y. Ma, G. Zhao, R. Alderliesten, On the mix-mode fracture of carbon fibre/epoxy composites interleaved with various thermoplastic veils, Compos. Commun. 33 (2022) 101230.
[23] M.B.M. Rehan, J. Rousseau, S. Fontaine, X.J. Gong, Experimental study of the influence of ply orientation on DCB mode-I delamination behavior by using multidirectional fully isotropic carbon/epoxy laminates, Compos. Struct. 161 (2017) 1–7.
[24] R. Frassine, A. Pavan, Viscoelastic effects on the interlaminar fracture behaviour of thermoplastic matrix composites: I. Rate and temperature dependence in unidirectional PEI/carbon-fibre laminates, Compos. Sci. Technol. 54 (2) (1995) 193–200.
[25] R. Akkerman, P.E. Reed, K.Y. Huang, L. Warnet, Comparison of Fracture Toughness (GIC) Values of Polyetherimide (PEI) and a carbon-fibre/PEI composite: an Experimental and Theoretical Study, 27, European Structural Integrity Society, 2000, pp. 3–14.
[26] Q. Voleppe, W. Ballout, P. Van Velthem, C. Bailly, T. Pardoen, Enhanced fracture resistance of thermoset/thermoplastic interfaces through crack trapping in a morphology gradient, Polymers 218 (2021) 123497.
[27] M.T. Heitzmann, M. Hou, M. Veidt, L.J. Vandi, R. Paton, Morphology of an interface between polyetherimide and epoxy prepreg, Adv. Mat. Res. 393 (2012) 184–188.
[28] P. Bruckbauer, U. Beier, K. Drechsler, Polyetherimid-epoxidharz interphasen zur anbindung von funktionsschichten auf faserverbundwerkstoffen, Z. Kunststofftechnik 14 (1) (2018) 35–56.
[29] J. Teuwen, J. Asquier, P. Inderkum, K. Masania, C. Brauner, I. Fernandez Villegas, C. A. Dransfeld, Gradient interphases between high-Tg epoxy and polyetherimide for advanced joining processes. In *Proceedings of the 18th European Conference on Composite Materials: 24-28th June* 2018, Athens, Greece, https://pure.tudelft.nl/ws/portalfiles/portal/47536817/1213_811_Dransfeld_Clemens.pdf.